Supplementary Material

The hypouricemic and renal protective effects of the Chinese functional tea *Ligustrum robustum* on hyperuricemic mice

Contents	Page

Table S1. PCR primer sequences and protocols.

Gene	Sense primer(5′- 3′)	Antisense primer(5′- 3′)	Product size (bp)	Tm(℃)
Ccl5	CCAAGTGTGTGCCAACCCAGA	ATGCCCATTTTCCCAGGACCG	191	60
Edn1	TGACGCACAACCGAGCACAT	TGGTCCTCTGCCCGTCTGAA	169	60
Mmp3	TGGGCTATACGAGGGCACGA	TTCACGGTTGCAGGGAGACC	77	60
Socs3	ACCCAGTCGGGGACCAAGAA	GGTTCCGTGGGTGGCAAAGA	173	60
Spi1	ATGTCAAGGGAGGGGGCTCA	ATCCCCCTCAGGACCAGGTG	115	60
Fos	TTCAACGCCGACTACGAGGC	GGAGATGGCTGTCACCGTGG	189	60
Nr4a1	AGAGACGCGAGTGCAGCC	ACTCAAGGGCCAGGGGATCA	238	60
Gapdh	CCTCGTCCCGTAGACAAAATG	TGAGGTCAATGAAGGGGTCGT	133	60

Table S2. The weight, fractionation rate, dosing amount, and normalization ratio of each eluted fraction from LR.

Eluted Fractions	Weight (g)	Fractionation Rate (%)	Dosing Amount (mg/kg)	Normalization Ratio
W1	30.1	40.13%	220.47	1
W2	6.06	8.08%	44.39	4.97
25%MW	9.27	12.36%	67.91	3.25
35%MW	9.17	12.23%	67.19	3.28
50%MW	7.31	9.75%	53.57	4.12
60%MW	4.98	6.64%	36.48	6.04
70%MW	6.77	9.03	49.61	4.44

Table S3. MRM parameters of 2 components and internal standards.

Compounds	Precursor	Production	Fragmentor(V)	CE(V)	CAV(V)
Verbascoside	623.2 $[M-H]^-$	461.2	145	20	5
Ligupurpuroside A	769.2 $[M-H]^-$	607.0	160	20	5
Naringenin (ISTD)	271.1 $[M-H]^-$	150.8	114	14	5

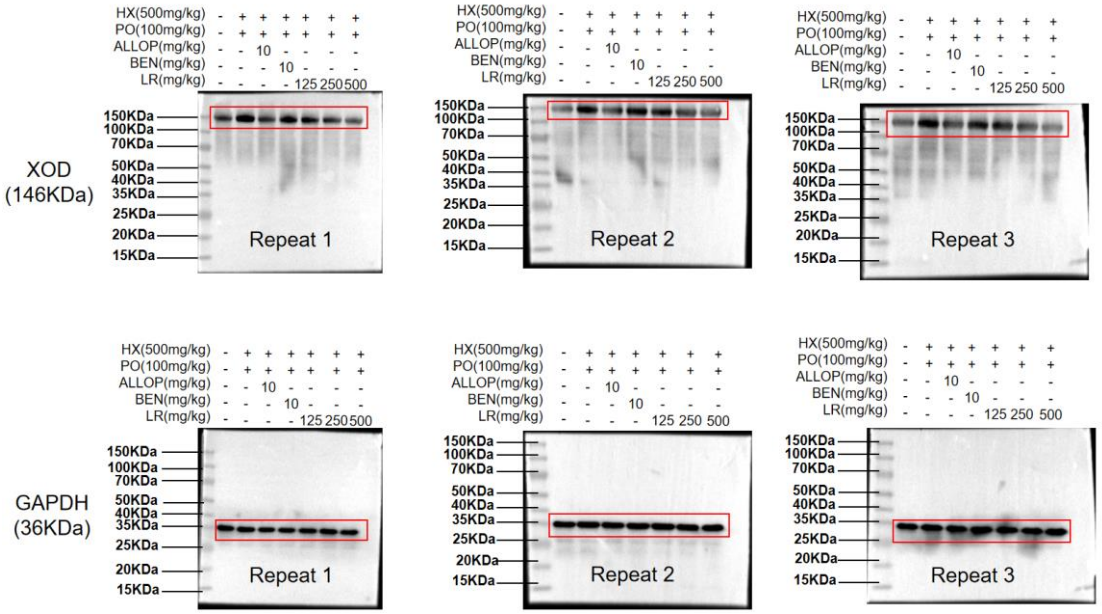

Fig. S1. Triplicate original XOD protein imprinting images of the Western blot analysis.

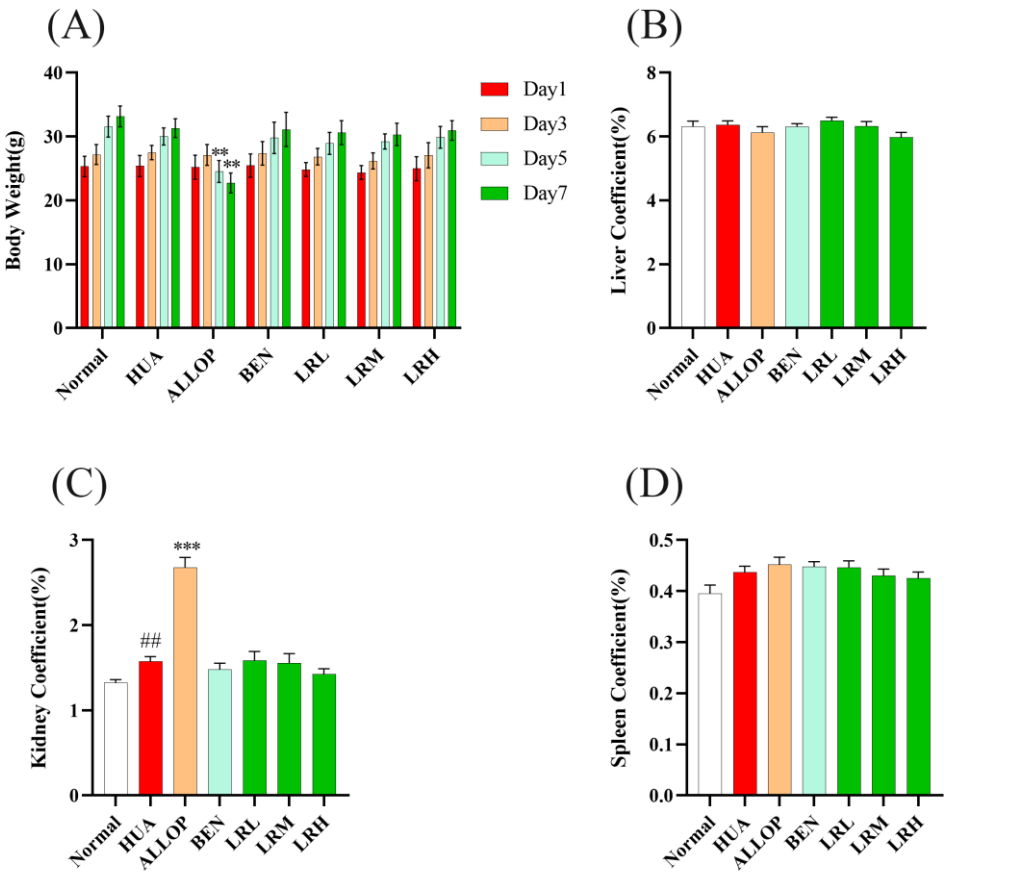

Fig. S2. Effects of LR on (A) body weight, and (B) liver, (C) kidney, and (D) spleen coefficients. The data were presented as the means ± SEMs (n=10). $^{\#\#}p < 0.01$ vs Normal; $^{**}p < 0.01$, $^{***}p < 0.001$ vs HUA.

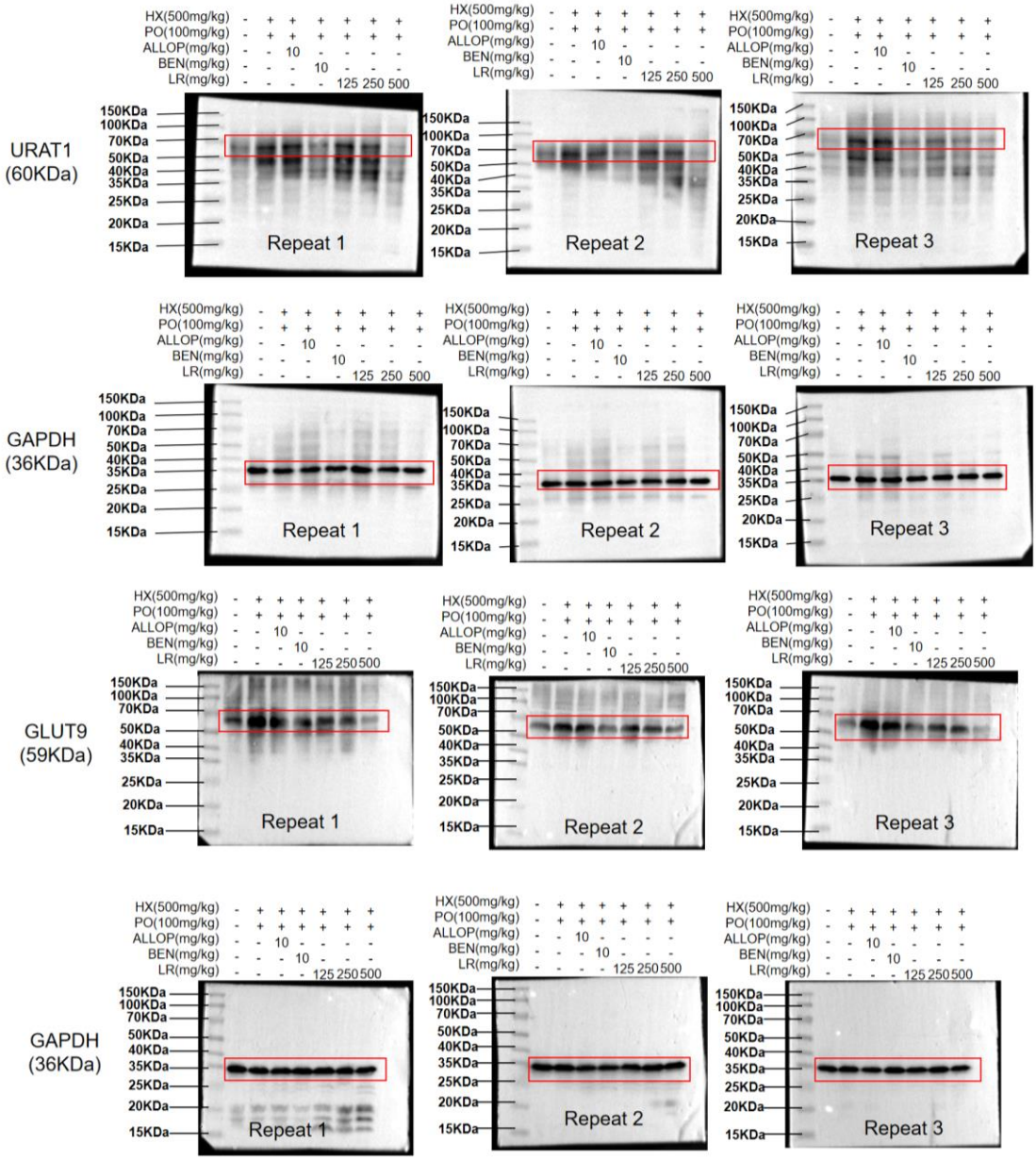
URAT1
(60KDa)
GAPDH
(36KDa)
GLUT9
(59KDa)
GAPDH
(36KDa)
HX(500mg/kg)
PO(100mg/kg)
ALLOP(mg/kg)
BEN(mg/kg)
LR(mg/kg)
125 250 500
150KDa
100KDa
70KDa
50KDa
40KDa
35KDa
25KDa
20KDa
15KDa
Repeat 1
Repeat 2
Repeat 3

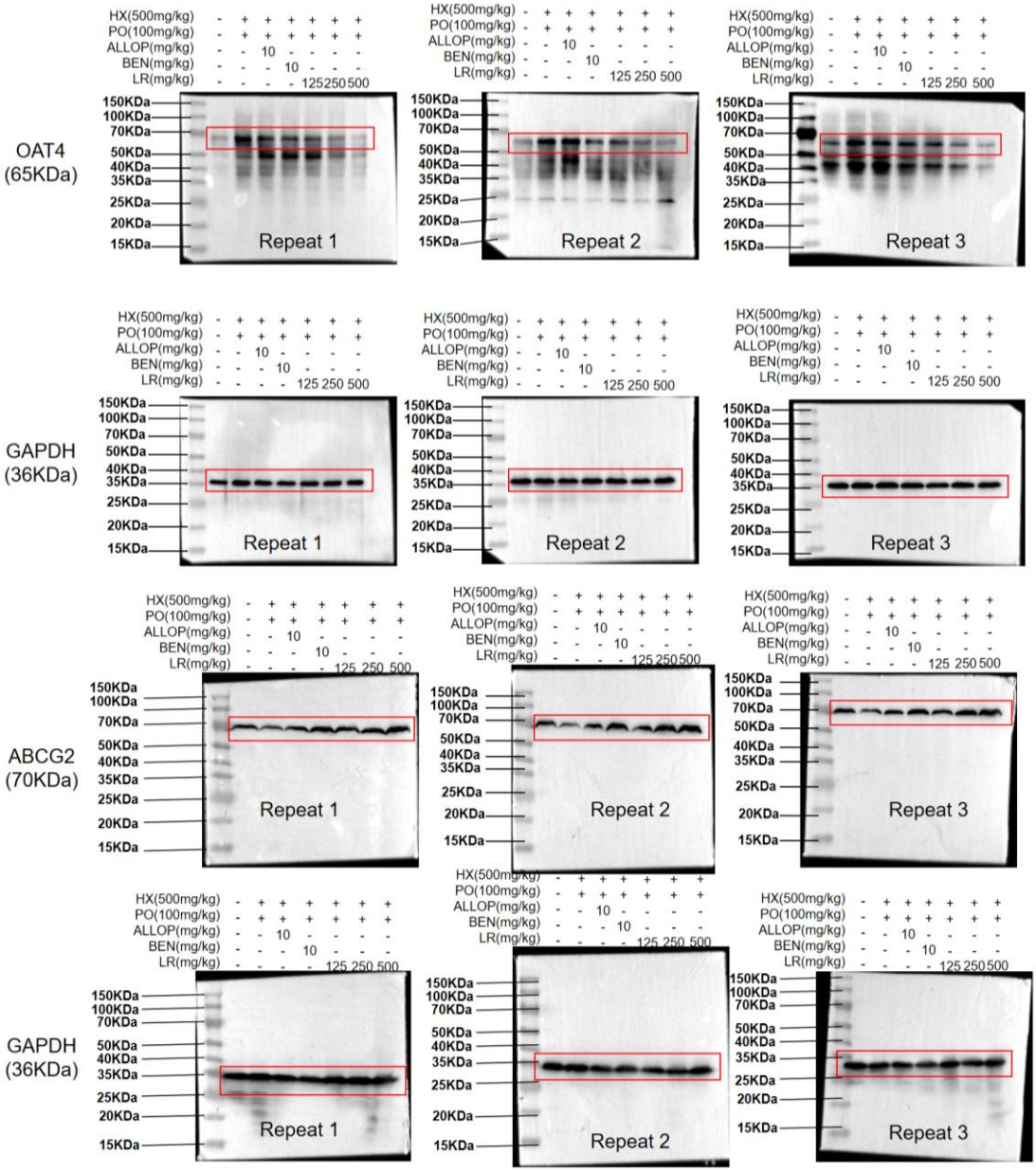
OAT4
(65KDa)
GAPDH
(36KDa)
ABCG2
(70KDa)
GAPDH
(36KDa)
HX(500mg/kg)
PO(100mg/kg)
ALLOP(mg/kg)
BEN(mg/kg)
LR(mg/kg)
125 250 500
150KDa
100KDa
70KDa
50KDa
40KDa
35KDa
25KDa
20KDa
15KDa
Repeat 1
Repeat 2
Repeat 3

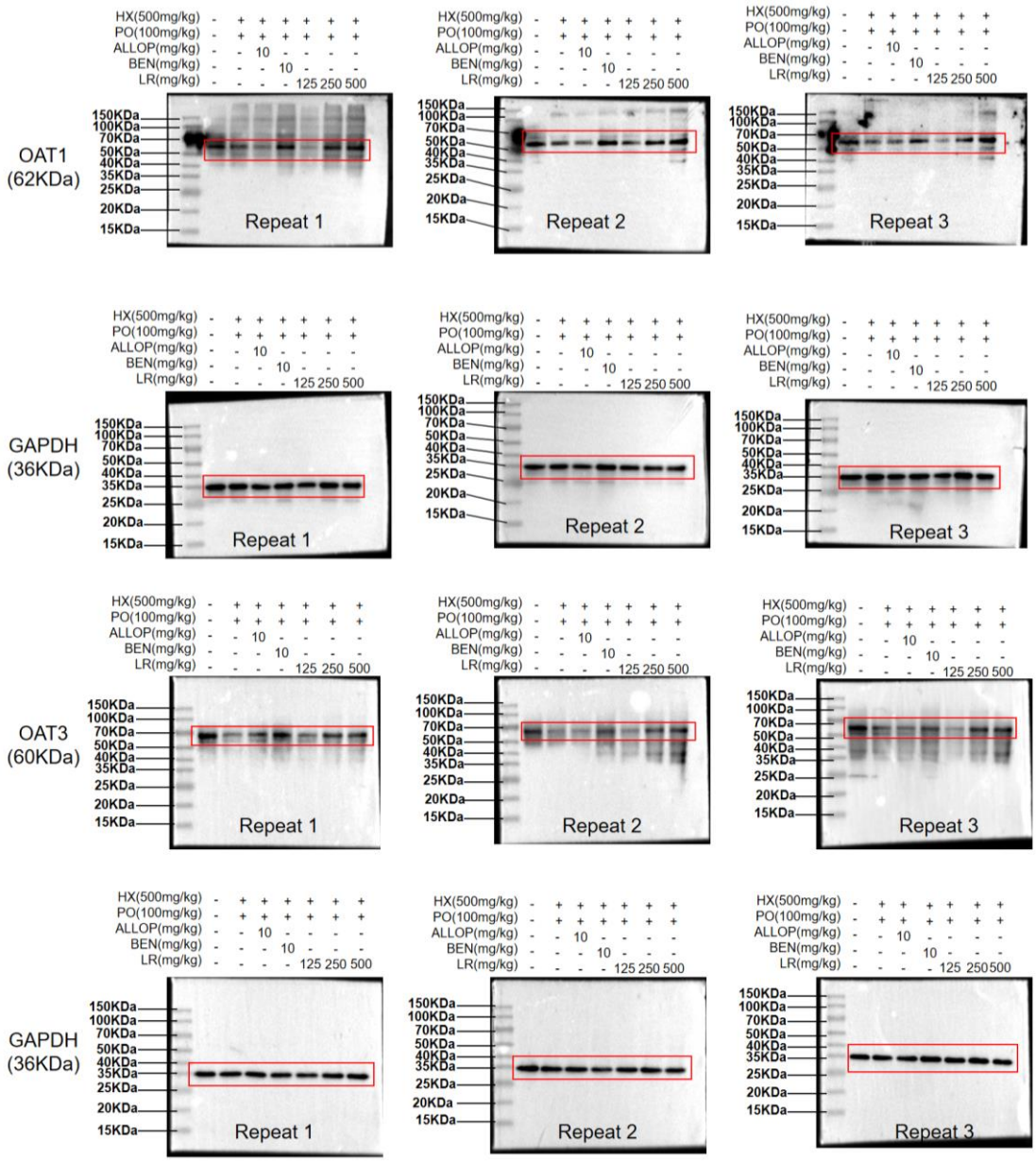

Fig. S3. Triplicate original URAT1, GLUT9, OAT4, ABCG2, OAT1, OAT3 protein imprinting images of the Western blot analysis.

Table S4. Quality analysis of transcriptome sequencing data of different samples.

Sample	Raw reads	Clean reads	Clean bases	Error (%)	Q20(%)	Q30(%)	GC(%)
Normal 1	49494494	49248520	7.32G	0.01	98.71	95.93	48.76
Normal 2	47857394	47599446	7.07G	0.01	98.66	95.8	48.89
Normal 3	48931152	48665592	7.24G	0.01	98.61	95.65	48.78
LRH 1	52170050	51850082	7.7G	0.01	98.56	95.5	48.34
LRH 2	44588840	44312118	6.57G	0.01	98.59	95.64	48.63
LRH 3	54473448	54148372	8.04G	0.01	98.52	95.37	49.08
HUA 1	52840408	52513708	7.83G	0.01	98.53	95.4	49.9
HUA 2	54296352	53940972	8.02G	0.01	98.58	95.56	49.56
HUA 3	52225008	51877140	7.72G	0.01	98.56	95.51	49.86

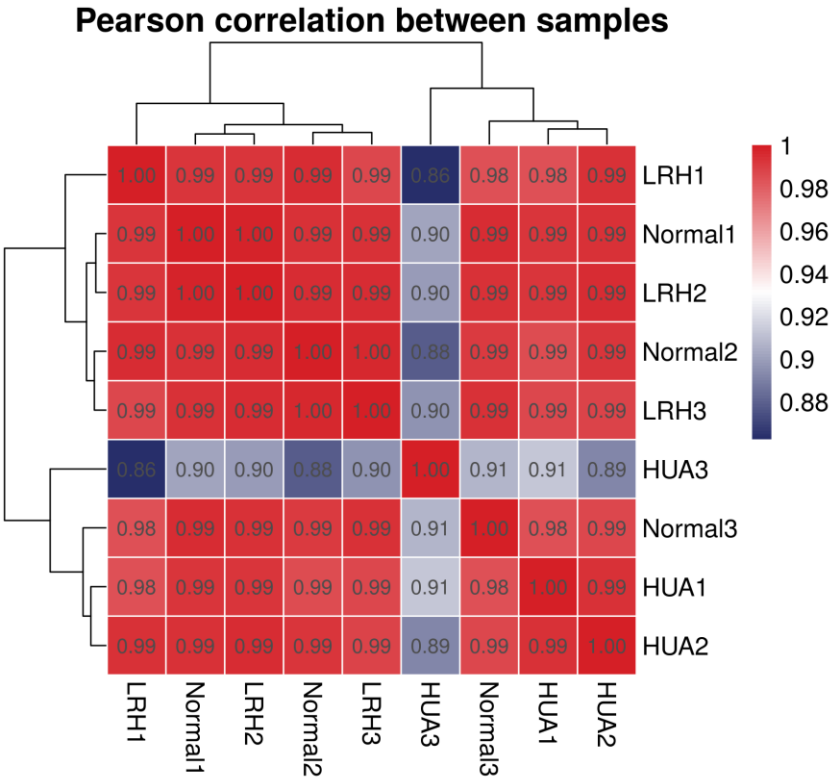

Fig. S4. Correlation thermograms between samples in different groups.

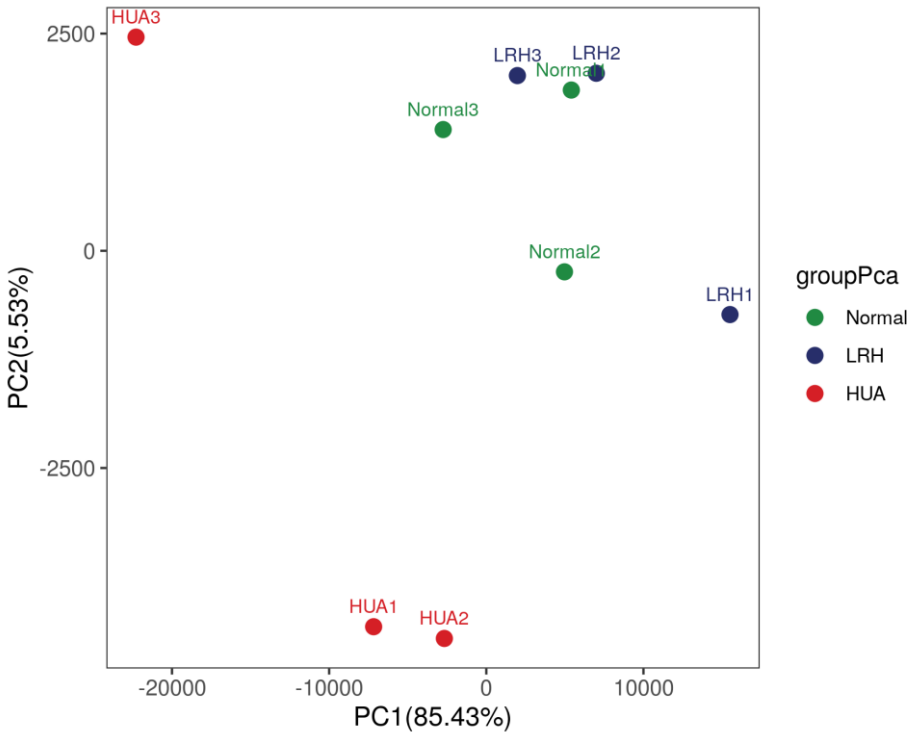

Fig. S5. Principal component analysis of individual replicates.

Table S5. FPKM values of 41 transcriptome-derived DEGs reversed by LRH.

DEGs	FPKM		
	Normal	HUA	LRH
Abca4	2.73 ± 1.58	1.25 ± 0.72	2.45 ± 1.42
Adipoq	0.09 ± 0.05	0.56 ± 0.32	0.04 ± 0.02
Alb	0.92 ± 0.53	0.45 ± 0.26	1.99 ± 1.15
Casq1	0.49 ± 0.28	1.81 ± 1.05	0.33 ± 0.19
Ccl5	2.05 ± 1.19	6.06 ± 3.5	0.61 ± 0.35
Ccr2	0.64 ± 0.37	3.5 ± 2.02	0.44 ± 0.25
Cd14	8.07 ± 4.66	47.58 ± 27.47	4.78 ± 2.76
Cfi	3.32 ± 1.92	23.22 ± 13.41	2.7 ± 1.56
Ctla4	0.01 ± 0	0.2 ± 0.12	0.01 ± 0.01
Dnai1	0.05 ± 0.03	0.2 ± 0.11	0.04 ± 0.02
Edn1	1.25 ± 0.72	3.32 ± 1.92	1.12 ± 0.65
Fbn1	3.17 ± 1.83	6.73 ± 3.88	1.13 ± 0.65
Fkbp10	3.09 ± 1.78	6.69 ± 3.86	1.8 ± 1.04

Gal	0 ± 0	0.21 ± 0.12	0 ± 0
Havcr1	1.44 ± 0.83	130 ± 75.06	4.14 ± 2.39
Hmgcs2	7.03 ± 4.06	2.93 ± 1.69	5.93 ± 3.42
Hp	0.68 ± 0.39	1.86 ± 1.08	0.58 ± 0.33
Irf4	0.12 ± 0.07	0.52 ± 0.3	0.1 ± 0.06
Itgam	0.09 ± 0.05	0.61 ± 0.35	0.04 ± 0.02
Itgb2	1.67 ± 0.96	4 ± 2.31	1.3 ± 0.75
Itgb3	0.65 ± 0.38	1.62 ± 0.94	0.47 ± 0.27
Krt18	27.63 ± 15.95	71.37 ± 41.2	24.77 ± 14.3
Lcn2	2.5 ± 1.44	49.29 ± 28.46	4.57 ± 2.64
Lgals1	78.29 ± 45.2	252.72 ± 145.91	73.43 ± 42.4
Lpl	55.14 ± 31.83	24.66 ± 14.24	45.95 ± 26.53
Lrrc66	10.84 ± 6.26	5.12 ± 2.96	9.44 ± 5.45
Mmp3	0.17 ± 0.1	1.34 ± 0.77	0.1 ± 0.06
Ngf	1.9 ± 1.1	4.49 ± 2.59	1.38 ± 0.8
Orm2	0.24 ± 0.14	1.47 ± 0.85	0.15 ± 0.09
Pdlim7	3.32 ± 1.92	7.58 ± 4.37	3.06 ± 1.77
Runx1	0.17 ± 0.1	0.68 ± 0.39	0.18 ± 0.1
Saa1	0.05 ± 0.03	0.84 ± 0.48	0.03 ± 0.02
Serpine1	0.45 ± 0.26	1.83 ± 1.06	0.55 ± 0.32
Serpinf1	1.07 ± 0.62	2.86 ± 1.65	0.87 ± 0.5
Socs3	1.57 ± 0.91	7.47 ± 4.31	1.12 ± 0.65
Sox9	0.31 ± 0.18	2.79 ± 1.61	0.22 ± 0.13
Syk	0.4 ± 0.23	1.05 ± 0.6	0.39 ± 0.22
Thbs4	0.17 ± 0.1	1.22 ± 0.7	0.08 ± 0.04
Timp1	0.8 ± 0.46	27.51 ± 15.88	0.36 ± 0.21
Tlr9	0.27 ± 0.16	0.81 ± 0.47	0.1 ± 0.06
Wnt4	1 ± 0.58	2.1 ± 1.21	0.32 ± 0.18

Table S6. Top 10 KEGG pathways enriched by the 41 DEGs.

Signaling pathways	Genes involved
Rheumatoid arthritis	Ccl5/Ctla4/Itgb2/Mmp3
Complement and coagulation cascades	Cfi/Itgam/Itgb2/Serpine1
Tuberculosis	Cd14/Itgam/Itgb2/Syk/Tlr9
Phagosome	Cd14/Itgam/Itgb2/Itgb3/Thbs4
TNF signaling pathway	Ccl5/Edn1/Mmp3/Socs3
Herpes simplex virus 1 infection	Ccl5/Itgb3/Socs3/Syk/Tlr9
Staphylococcus aureus infection	Cfi/Itgam/Itgb2/Krt18
Legionellosis	Cd14/Itgam/Itgb2
Acute myeloid leukemia	Cd14/Itgam/Runx1
Pertussis	Cd14/Itgam/Itgb2

Table S7. Transcription factors for key genes in the TNF/NF-κB signaling pathway.

TF	Spi1	Fos	Nr4a1
Key genes	Ccl5	Ccl5, Socs3	Edn1

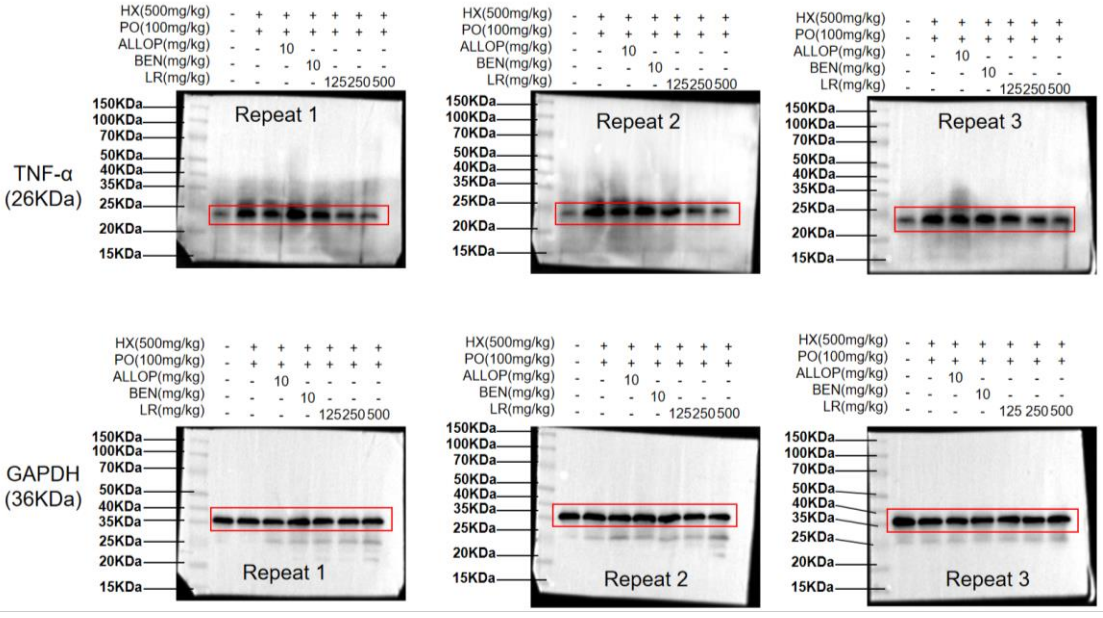

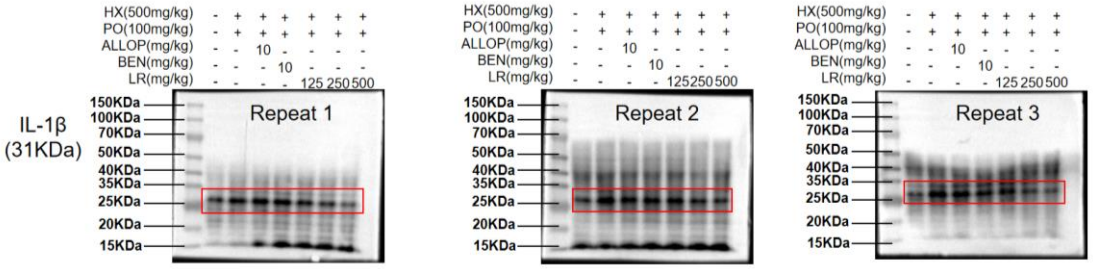
IL-1β
(31KDa)
HX(500mg/kg) - + + + + + +
PO(100mg/kg) - + + + + + +
ALLOP(mg/kg) - - 10 - - - -
BEN(mg/kg) - - - 10 - - -
LR(mg/kg) - - - - 125 250 500
150KDa
100KDa
70KDa
50KDa
40KDa
35KDa
25KDa
20KDa
15KDa
Repeat 1
Repeat 2
Repeat 3

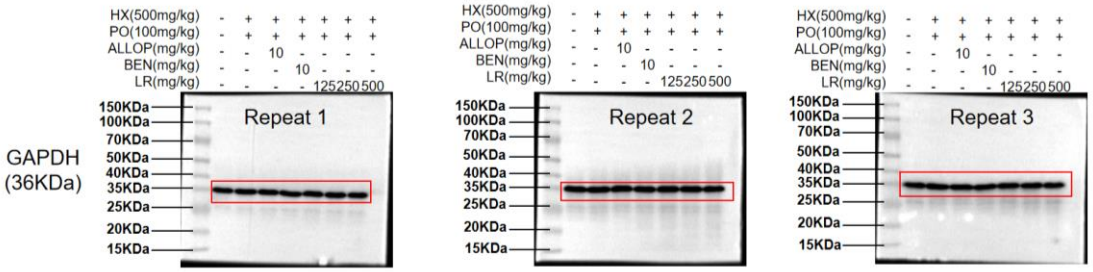
GAPDH
(36KDa)
HX(500mg/kg) - + + + + + +
PO(100mg/kg) - + + + + + +
ALLOP(mg/kg) - - 10 - - - -
BEN(mg/kg) - - - 10 - - -
LR(mg/kg) - - - - 125250500
150KDa
100KDa
70KDa
50KDa
40KDa
35KDa
25KDa
20KDa
15KDa
Repeat 1
Repeat 2
Repeat 3

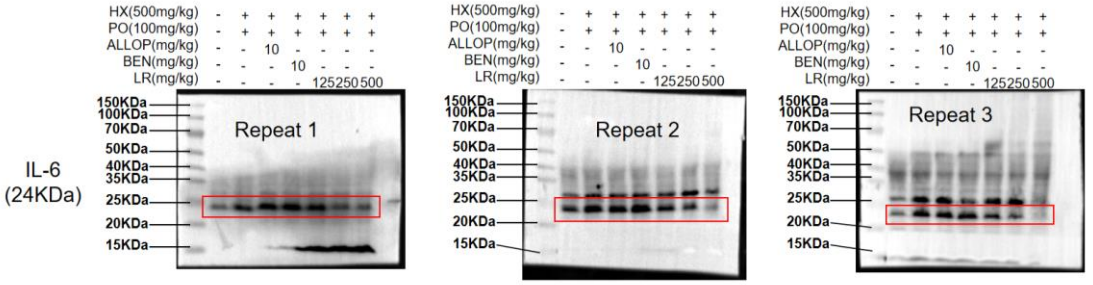
IL-6
(24KDa)
HX(500mg/kg) - + + + + + +
PO(100mg/kg) - + + + + + +
ALLOP(mg/kg) - - 10 - - - -
BEN(mg/kg) - - - 10 - - -
LR(mg/kg) - - - - 125250500
150KDa
100KDa
70KDa
50KDa
40KDa
35KDa
25KDa
20KDa
15KDa
Repeat 1
Repeat 2
Repeat 3

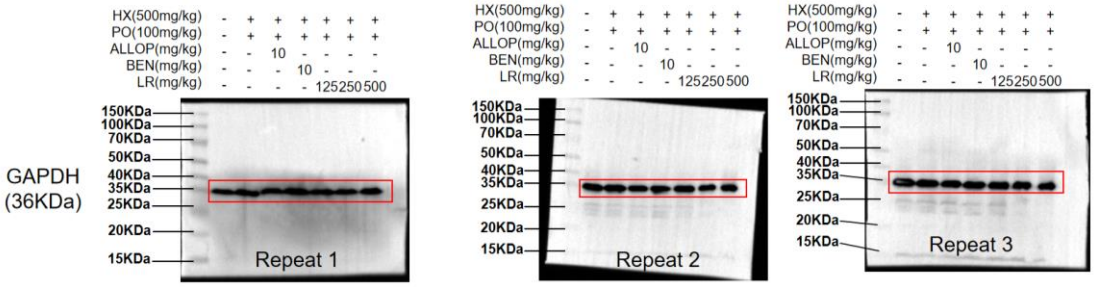
GAPDH
(36KDa)
HX(500mg/kg) - + + + + + +
PO(100mg/kg) - + + + + + +
ALLOP(mg/kg) - - 10 - - - -
BEN(mg/kg) - - - 10 - - -
LR(mg/kg) - - - - 125250500
150KDa
100KDa
70KDa
50KDa
40KDa
35KDa
25KDa
20KDa
15KDa
Repeat 1
Repeat 2
Repeat 3

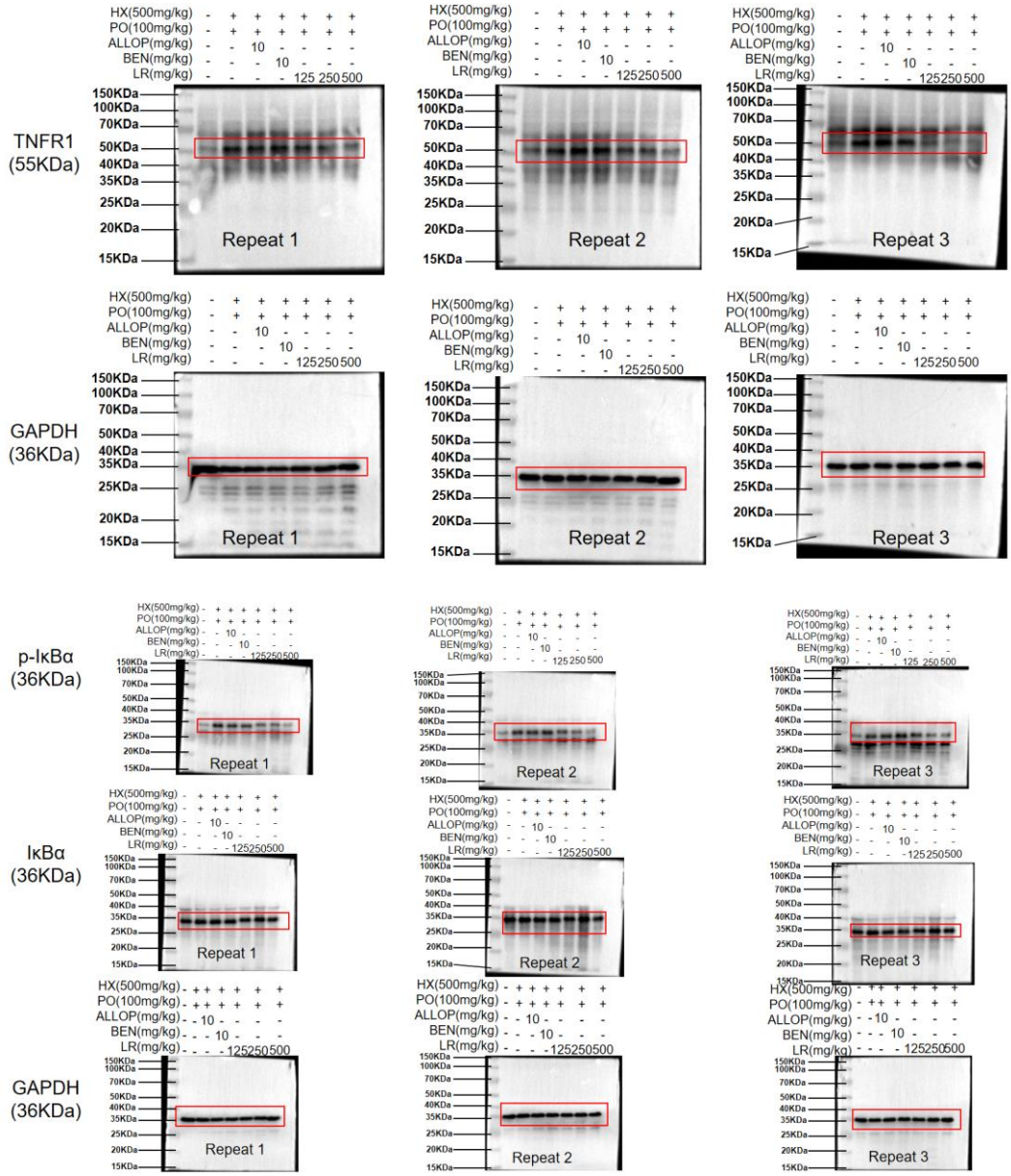
TNFR1
(55KDa)
GAPDH
(36KDa)
p-IκBα
(36KDa)
IκBα
(36KDa)
GAPDH
(36KDa)
HX(500mg/kg)
PO(100mg/kg)
ALLOP(mg/kg)
BEN(mg/kg)
LR(mg/kg)
150KDa
100KDa
70KDa
50KDa
40KDa
35KDa
25KDa
20KDa
15KDa
Repeat 1
Repeat 2
Repeat 3

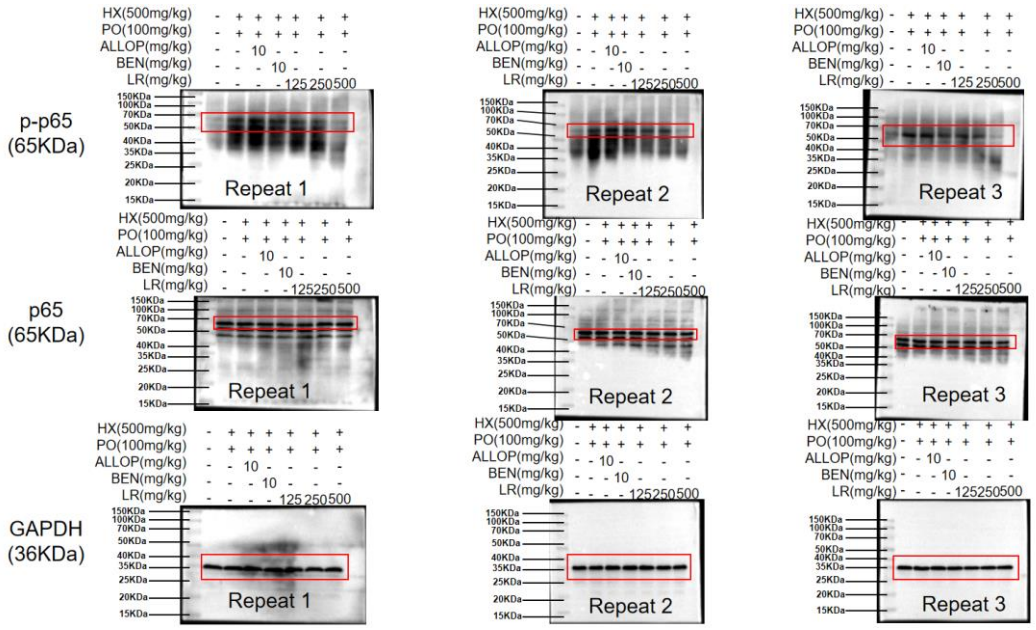

Fig. S6. Triplicate original TNF-α, IL-1β, IL-6, TNFR1, p-IκBα, IκBα, p-p65, p65 protein imprinting images of the Western blot analysis.

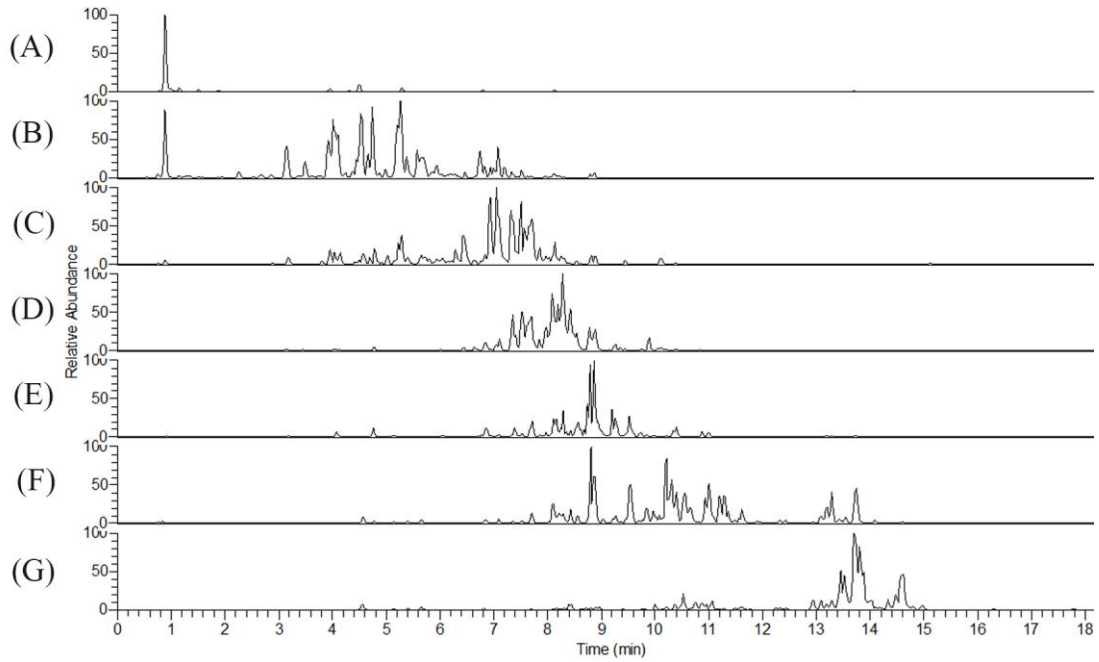

Fig. S7. The representative UHPLC-Q-Orbitrap HRMS base peak chromatogram (BPC) of the respective fractions. W1 (A), W2 (B), 25%MW (C), 35%MW (D), 50%MW (E), 60%MW (F), 70%MW (G).

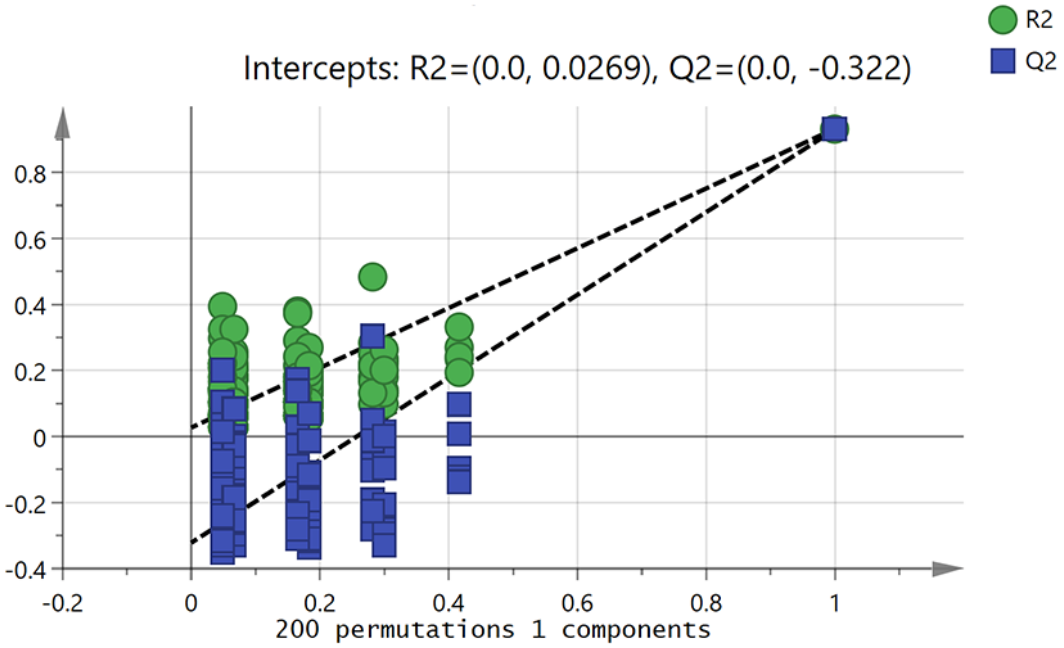

Fig. S8. Permutation test validation plot of the OPLS model.

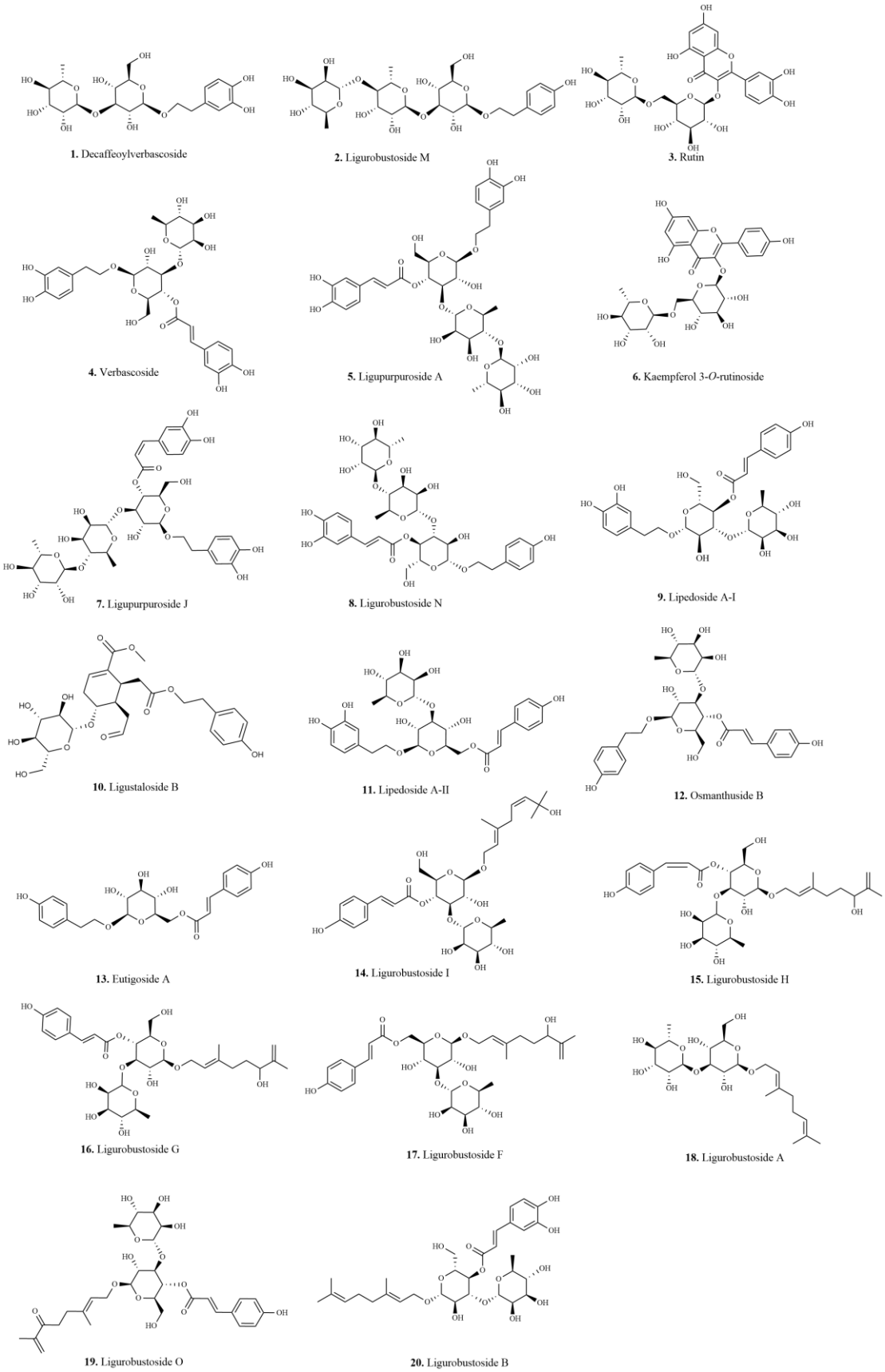

Fig. S9. Chemical structures of the 20 putative active compounds.

Table S8. 20 putative active components from LR: VIP values, RC values, and binding energies with XOD.

ID	Compound	VIP	RC	Bind Energy (kcal/mol)
1	Decaffeoylverbascoside	1.10	1.49E-06	-8.8
2	Ligurobustoside M	1.77	2.31E-06	-9.2
3	Rutin	2.54	9.05E-07	-9.6
4	Verbascoside	1.44	6.00E-08	-9.5
5	Ligupurpuroside A	6.76	8.42E-06	-9.8
6	Kaempferol 3-O-rutinoside	1.12	1.70E-06	-9.6
7	Ligupurpuroside J	1.65	1.92E-06	-9.5
8	Ligurobustoside N	1.94	2.30E-06	-9.7
9	Lipedoside A-I	3.17	4.09E-06	-9.5
10	Ligustaloside B	1.02	4.41E-07	-7.4
11	Lipedoside A-II	1.69	2.09E-06	-9.6
12	Osmanthuside B	1.35	1.68E-06	-9.5
13	Eutigoside A	1.11	7.11E-07	-9.2
14	Ligurobustoside I	1.19	7.93E-07	-9
15	Ligurobustoside H	1.64	4.18E-06	-7.9
16	Ligurobustoside G	1.46	3.19E-06	-9
17	Ligurobustoside F	2.87	1.05E-06	-8.8
18	Ligurobustoside A	1.01	3.61E-07	-8.7
19	Ligurobustoside O	1.34	9.43E-07	-9
20	Ligurobustoside B	2.62	9.58E-07	-8.9
21	Allopurinol	-	-	-6.5
22	Febuxostat	-	-	-8.9

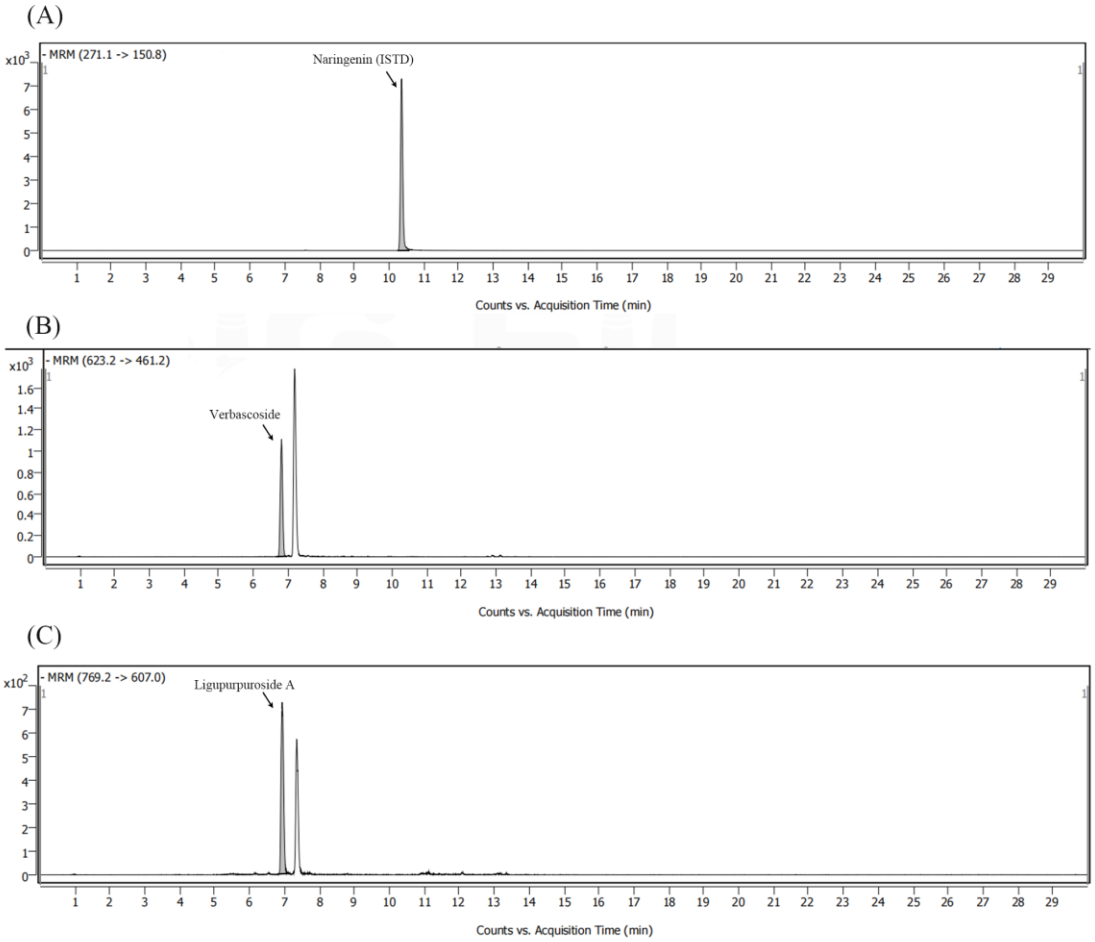

Fig. S10. Quantitative determination of compounds verbascoside (**4**) and ligupurpuroside A (**5**) by LC-MS. The MRM chromatograms of (A) naringenin (ISTD), (B) verbascoside , and (C) ligupurpuroside A in the LR.

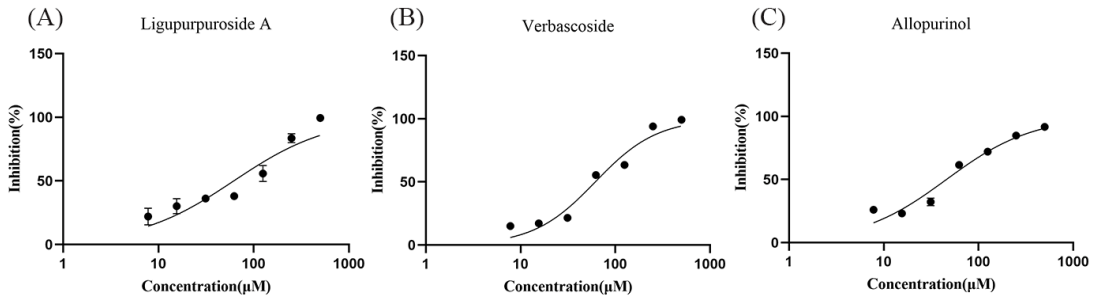

Fig. S11. Inhibitory effects of ligupurpuroside A, verbascoside, and allopurinol on XOD activity in *vitro*. The dose-response curves were fitted by nonlinear regression, and the half-maximal inhibitory concentration (IC_{50}) values were calculated. Data are presented as the mean ±SEM of three independent experiments.

1. Experimental Section

1.1 Induction of HUA and treatment with drugs

Mice were fed a standard laboratory chow diet and had free access to water throughout the experiment. Body weight was recorded at the beginning and end of the experiment. Excluding the Normal control group, the remaining mice were subjected to HUA induction over seven consecutive days by receiving PO (300 mg/kg/day) via intraperitoneal injection and HX (500 mg/kg/day) via oral gavage. On the third day of the experiment, the treatment groups was subjected to administration of the corresponding drugs. On the sixth experimental day, urine was collected from each group after dosing. Subsequently, on the seventh experimental day, blood was drawn from all mice following administration. Following collection, the blood was allowed to clot for 60 minutes. The samples were then centrifuged at 3000 rpm (4 °C) for 10 minutes to isolate the serum. Urine samples were processed under the same conditions to collect supernatants. Serum and urine supernatants were aliquoted for biochemical analysis, including measurements of UA, XOD, CRE, and BUN activity. For downstream analysis including H&E staining, Western blot, RT-qPCR, and transcriptomic analysis, the collected tissues were immediately frozen and archived at -80 °C.

The hyperuricemia model was established by co-administration of potassium oxonate (PO) and hypoxanthine (HX) for 7 days. This combined model is a well-recognized, widely used pharmacological hyperuricemia model in urate-lowering research, enabling rapid and reproducible induction of hyperuricemia for initial screening of functional food ingredients. Although it represents an acute pharmacological model rather than chronic multifactorial human hyperuricemia, it remains the most prevalent choice for evaluating urate-lowering efficacy and renal protection of natural products in preclinical studies.

1.2 Western blot analysis

Western blotting was utilized to determine LR's effect on XOD expression in the liver, alongside quantifying the levels of UA transporters and pathway-related proteins in kidney tissue. Tissue proteins were extracted and quantified (using the BCA method).

Afterwards, protein denaturation was performed. Next, the protein samples underwent separation via Sodium Dodecyl Sulfate-Polyacrylamide Gel Electrophoresis (SDS-PAGE), followed by transfer to a membrane and exposure to a blocking solution. The membranes were then incubated with the primary antibodies overnight at 4 °C: XOD, GAPDH (1:10000); URAT1, GLUT9, OAT1, OAT4, and ABCG2 (1:3000); TNF-α, IL-1, IL-6, TNFR1, p-p65, p65, p-IκBα, and IκBα (1:5000). The membranes were then washed with the same volume of TBST and co-incubated with the corresponding secondary antibodies for 2 hours. The resulting fluorescent signals from the protein bands, generated via enhanced chemiluminescence, were captured and determined using an imaging system (Tanon, China). Protein levels were determined by the gray value analysis using Image J software.

1.3 RT–qPCR analysis

The 20 μL reaction mixture was prepared using 10 μL of BrightCycle Universal SYBR Green qPCR Mix (containing UDG), 2 μL of cDNA, 7.2 μL of dd-H2O, and 0.4 μL of both the forward and reverse primers. The qPCR thermal profile included an initial denaturation phase (95 °C for 3 min), succeeded by 40 cycles of amplification (95 °C for 5 s and 60 °C for 30–34 s).

1.4 Molecular dynamics simulation

Molecular dynamics (MD) simulation was performed for XOD-ligupurpuroside A utilizing Amber 24 software. The protein was assigned to the Amber ff99 force field. The TIP3P explicit solvent model was implemented to solvate the protein system via the leap module, with the system geometry defined as a regular dodecahedron. The minimum distance between the solvent boundary and the protein structure was set to 15 Å. Cl^- were introduced to neutralize the system, achieving a net charge of zero, thereby establishing the protein-solvent system. Periodic boundary conditions (PBC) were applied to the model to eliminate boundary artifacts. Following energy minimization of the system, the NPT ensemble (isothermal and isobaric) was employed to heat the system from 10 K to 300 K at constant volume over a duration of 100 ps. Subsequent to this, a 500 ps equilibrium simulation was conducted. Finally, the SHAKE algorithm was utilized to constrain the stretching of chemical bonds involving hydrogen

atoms. The integration time step of the simulation was set to 2 fs, and all restraints imposed on the system were released to initiate the production MD run. The simulation process was accelerated on Graphics Processing Units (GPUs) via compilation with the pmemd.cuda program.

Trajectory processing of the simulation was performed using the Amber traj program. Conformations of the simulated system were outputted at 2 fs intervals. The Root Mean Square Deviation (RMSD) and Root Mean Square Fluctuation (RMSF) were calculated for the complex system, protein Cα atoms, receptor backbone, and small molecule, respectively. The Grace software was employed for the visualization of output conformations. MD trajectories were generated using the traj program, and the MMGBSA.py script was utilized to compute the average binding energy. Specifically, 50 conformations were selected from the stable phase (80–100 ns) of the trajectories where the RMSD fluctuated within 3 Å, with one frame extracted every 4 frames for the calculation.

1.5 Determination of XOD inhibitory activity

Into a 96-well plate, 100 μL of the test sample and 50 μL of the 0.1 U/mL XOD solution were dispensed. The plate was subsequently oscillated for 30 seconds and then incubated at 25°C for 5 minutes. Next, 50 μL of the 600 μmol/L xanthine solution was introduced into the plate. Following 30 seconds of oscillation, the initial absorbance reading at 290 nm (A1) was promptly recorded. After further incubation for 25 minutes, the absorbance at 290 nm was measured again (A_2). The percentage of XOD inhibition was determined according to the following formula: Inhibition rate (%) = [1 − (A_2 − A_1) of drug group / (A_2 − A_1) of blank group] × 100%.